2014

Equatorial Pacific coral geochemical records show recent weakening of the Walker Circulation

Jessica E. Carilli
Australian Nuclear Science and Technology Organisation

Helen V. McGregor
Australian National University, mcgregor@uow.edu.au

Jessica J. Gaudry
University of Wollongong, jgaudry@uow.edu.au

Simon D. Donner
University of British Columbia

Michael K. Gagan
Australian National University

See next page for additional authors

Equatorial Pacific coral geochemical records show recent weakening of the Walker Circulation

Abstract

Equatorial Pacific ocean-atmosphere interactions affect climate globally, and a key component of the coupled system is the Walker Circulation, which is driven by sea surface temperature (SST) gradients across the equatorial Pacific. There is conflicting evidence as to whether the SST gradient and Walker Circulation have strengthened or weakened over the late twentieth century. We present new records of SST and sea surface salinity (SSS) spanning 1959-2010 based on paired measurements of Sr/Ca and δ18O in a massive Porites coral from Butaritari atoll in the Gilbert Islands, Republic of Kiribati, in the central western equatorial Pacific. The records show 2-7 year variability correlated with the El Niño-Southern Oscillation (ENSO) and corresponding shifts in the extent of the Indo-Pacific Warm Pool, and decadal-scale signals related to the Pacific Decadal Oscillation and the Pacific Warm Pool Index. In addition, the Butaritari coral records reveal a small but significant increase in SST (0.39°C) from 1959 to 2010 with no accompanying change in SSS, a trend that persists even when ENSO variability is removed. In contrast, larger increases in SST and SSS are evident in coral records from the equatorial Pacific Line Islands, located east of Butaritari. Taken together, the equatorial Pacific coral records suggest an overall reduction in the east-west SST and SSS gradient over the last several decades, and a recent weakening of the Walker Circulation.

Disciplines
Medicine and Health Sciences | Social and Behavioral Sciences

Authors
Jessica E. Carilli, Helen V. McGregor, Jessica J. Gaudry, Simon D. Donner, Michael K. Gagan, Samantha Stevenson, Henri Wong, and David Fink

RESEARCH ARTICLE

Key Points:
- A Pacific coral records slight ocean warming, no salinity change from 1959 to 2010
- Cross-Pacific coral records support recent Walker Circulation weakening
- Decadal-scale variability dominates central Pacific SST and salinity

Supporting Information:
- Readme
- Figure S1
- Figure S2
- Figure S3
- Table S1
- Table S2
- Text S1

Correspondence to:
J. E. Carilli,
jcarilli@gmail.com

Equatorial Pacific coral geochemical records show recent weakening of the Walker Circulation

Jessica E. Carilli[1,2], Helen V. McGregor[3], Jessica J. Gaudry[4], Simon D. Donner[5], Michael K. Gagan[3], Samantha Stevenson[6], Henri Wong[1], and David Fink[1]

[1]Institute for Environmental Research, Australian Nuclear Science and Technology Organization, Lucas Heights, New South Wales, Australia, [2]Now at School of the Environment, University of Massachusetts Boston, Boston, Massachusetts, USA, [3]Research School of Earth Sciences, Australian National University, Canberra, Australian Capital Territory, Australia, [4]School of Earth and Environmental Sciences, University of Wollongong, Wollongong, New South Wales, Australia, [5]Department of Geography, University of British Columbia, Vancouver, British Columbia, Canada, [6]Department of Oceanography, University of Hawaii, Honolulu, Hawaii, USA

Abstract Equatorial Pacific ocean-atmosphere interactions affect climate globally, and a key component of the coupled system is the Walker Circulation, which is driven by sea surface temperature (SST) gradients across the equatorial Pacific. There is conflicting evidence as to whether the SST gradient and Walker Circulation have strengthened or weakened over the late twentieth century. We present new records of SST and sea surface salinity (SSS) spanning 1959–2010 based on paired measurements of Sr/Ca and δ^{18}O in a massive *Porites* coral from Butaritari atoll in the Gilbert Islands, Republic of Kiribati, in the central western equatorial Pacific. The records show 2–7 year variability correlated with the El Niño–Southern Oscillation (ENSO) and corresponding shifts in the extent of the Indo-Pacific Warm Pool, and decadal-scale signals related to the Pacific Decadal Oscillation and the Pacific Warm Pool Index. In addition, the Butaritari coral records reveal a small but significant increase in SST (0.39°C) from 1959 to 2010 with no accompanying change in SSS, a trend that persists even when ENSO variability is removed. In contrast, larger increases in SST and SSS are evident in coral records from the equatorial Pacific Line Islands, located east of Butaritari. Taken together, the equatorial Pacific coral records suggest an overall reduction in the east-west SST and SSS gradient over the last several decades, and a recent weakening of the Walker Circulation.

1. Introduction

The El Niño–Southern Oscillation (ENSO) is the strongest mode of interannual climatic variability on Earth [*Wang et al.*, 1999]. The atmospheric Walker Circulation is an integral part of the ENSO system, and knowledge of its decadal and longer-scale variability is important for understanding ENSO variability [*England et al.*, 2014]. Under neutral conditions, an east-west sea surface temperature (SST) gradient exists between warm tropical waters in the western equatorial Pacific and the cooler waters to the east (Figure 1). This SST gradient is driven by coupling with the mean trade winds, which push warm equatorial surface waters toward the western Pacific, causing high sea surface dynamic heights and temperatures in the Western Pacific Warm Pool (WPWP) [*Cravatte et al.*, 2009]. The WPWP end of the SST gradient in turn contributes to the Walker Circulation, which is composed of rising moist air and corresponding intense rainfall in the western Pacific, and sinking dry air in the eastern Pacific. In addition to the east-west SST gradient, precipitation differences resulting from atmospheric ascent/descent lead to a sea surface salinity (SSS) gradient, with fresher waters in the west [*Delcroix and Picaut*, 1998]. Under La Niña conditions, the trade winds and Walker Circulation strengthen, upwelling increases in the east, the east-west SST gradient increases, and rainfall increases in the west and decreases in the eastern and central Pacific. The opposite set of ocean-atmosphere interactions occur during El Niño conditions [*Rasmusson and Wallace*, 1983].

WPWP dynamics and ENSO are inextricably linked, and there is evidence that the WPWP is becoming warmer and fresher and expanding to the east [*Delcroix et al.*, 2007; *Cravatte et al.*, 2009] and that a warmer WPWP causes stronger El Niño events [*Sun*, 2003]. *Vecchi et al.* [2006] and *Vecchi and Soden* [2007] suggest that as the climate warms, the hydrological cycle will intensify, but that warming should also cause a slowdown of the Walker Circulation due to an imbalance between increases in precipitation and saturation relative humidity. Global warming causes an increase in atmospheric moisture, but a smaller rate of increase in rainfall.
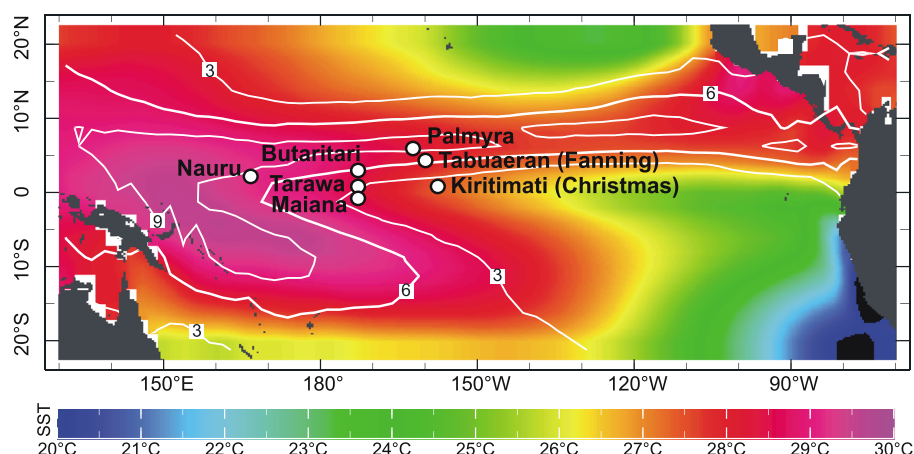
Figure 1. Location of the study area and distribution of equatorial Pacific rainfall and sea surface temperature (SST). Monthly Global Precipitation Climatology Project v2 (GPCPv2) combined satellite-gauge rainfall data (contours in mm/d) [*Adler et al.*, 2003] and extended reconstructed SST version 3b (ERSSTv3b) data for 1979–2010 (colors) [*Smith et al.*, 2008]. Locations of islands with coral core records from Nauru, the Gilbert Islands (including Butaritari) and the Line Islands chains are indicated (white circles).

This requires a reduction in atmospheric circulation, which is manifest as a reduction in the Walker Circulation [*Vecchi and Soden*, 2007]. However, attempts to test this hypothesis using observational data have produced conflicting results. *Tokinaga et al.* [2012] found a reduced east-west SST and nighttime air temperature gradient from observational data spanning 1950–2009, and weakened Walker Circulation using atmospheric models incorporating these data. Using stable nitrogen and carbon isotopes from proteinaceous corals offshore Palau, *Williams and Grottoli* [2010] found evidence for thermocline shoaling since the 1970s, also suggesting a weakening Walker Circulation. In contrast to these studies, *Solomon and Newman* [2012] removed ENSO variability from SST data products and found an increase in the east-west SST gradient and no evidence for a weakening Walker Circulation, and *Meng et al.* [2012] found evidence for a strengthening Walker Circulation using an atmospheric general circulation model and SST observations.

The discrepancies in observational studies of twentieth century climate trends may be related to limitations of the tropical Pacific Ocean data [*Deser et al.*, 2010]. Paleoclimate proxies are a good means for obtaining additional data to reduce the overall uncertainties. In particular, reconstructions of SST from Sr/Ca ratios in corals [e.g., *Beck et al.*, 1992] and seawater oxygen isotope ratios ($\Delta\delta^{18}O$, a proxy for SSS [e.g., *McCulloch et al.*, 1994; *Gagan et al.*, 1998; *Ren et al.*, 2003; *Cahyarini et al.*, 2008]) are uniquely suited for reconciling these discrepancies in observational data.

Coral records have the advantage of providing continuous, high-resolution (monthly or better) data from undersampled locations in the tropics. Coral-based records of SST and SSS from the Line Islands, central equatorial Pacific, showed that both warming and freshening occurred between 1972 and 1998 [*Nurhati et al.*, 2009, 2011], but contemporaneous records from corals spanning the tropical Pacific are needed to test for changes in east-west gradients. Coral oxygen isotope ($\delta^{18}O$) records from Tarawa [*Cole et al.*, 1993] and Maiana [*Urban et al.*, 2000] in the Gilbert Islands at approximately 172°E also show warming and/or freshening trends, but records with paired measurements of Sr/Ca and $\delta^{18}O$ are needed to separate SST and SSS to complete the picture. Here we present Sr/Ca, $\delta^{18}O$, and $\Delta\delta^{18}O$ records spanning 1959–2010 from Butaritari atoll (3.2°N, 172.8°E) in the Gilbert Islands, north of Tarawa and Maiana (Figure 1). Our records suggest that SST has increased at Butaritari over this time period at a lower rate than in the Line Islands and that no freshening has occurred, supporting a weakening Walker Circulation.

2. Methods

2.1. Study Area

Butaritari atoll is part of the Gilbert Islands group of the Republic of Kiribati, located in the central Pacific at 3.2°N, 172.8°E (Figure 1). SST varies minimally on a seasonal timescale, from about 28 to 30°C, but has large interannual fluctuations of more than 4°C due largely to the El Niño–Southern Oscillation [*Donner*, 2011].

Table 1. Correlation Coefficients for Climatic Variables for Butaritari and Tarawa

	Butaritari Rainfall[a]	Niño4	Niño3	Tarawa Rainfall[a]
Butaritari rainfall[a]		0.34[e]	0.27[e]	0.55[e]
SODA salinity at Butaritari[b]	−0.06	−0.50[e]	−0.54[e]	−0.38[e]
Delcroix salinity at Butaritari[c]	−0.09[e]	−0.55[e]	−0.55[e]	−0.40[e]
SST at Butaritari[d]	0.29[e]	0.82[e]	0.40[e]	0.38[e]
SODA salinity at Tarawa[b]	−0.11[e]	−0.49[e]	−0.60[e]	−0.45[e]
Tarawa rainfall[a]	0.55[e]	0.57[e]	0.51[e]	

[a]Rainfall from the Kiribati Meteorological Service.
[b]SODA salinity from the Simple Ocean Data Assimilation [*Carton and Giese*, 2008].
[c]Delcroix salinity from *Delcroix et al.* [2011].
[d]SST from ERSSTv3B [*Smith et al.*, 2008].
[e]Coefficients with $p < 0.05$.

InButaritari, rainfall tends to peak in the early boreal spring (March and April) with the passage of the Intertropical Congervence Zone (ITCZ) from south to north [*Chen et al.*, 1994]. There is sometimes a second peak in the late boreal summer or early fall (August and September) as the ITCZ passes back south [*Chen et al.*, 1994]. Annual average rainfall is higher at Butaritari than at central Pacific islands closer to the equator, with mean annual precipitation of 3105 mm between 1947 and 2007 (Kiribati Meteorological Service), in part because the edge of the ITCZ rainfall band can remain over the more northerly Butaritari between the boreal spring and summer. Butaritari can also remain on the edge of the ITCZ year round if a split ITCZ develops. Rainfall is positively correlated with ENSO indices, increasing during El Niño and decreasing during La Niña (Table 1). Salinity products for the grid cell containing Butaritari from the Simple Ocean Data Assimilation (SODA) [*Carton and Giese*, 2008; *Delcroix et al.*, 2011] are negatively correlated with ENSO indices; however, rainfall and salinity products are not well correlated with each other at Butaritari, while rainfall at Tarawa, to the south, is well correlated with salinity data products (Table 1) [*Cole et al.*, 1993].

2.2. Coral Core Collection and Processing

The coral core used for this study was collected from a massive *Porites sp.* coral in May 2010 at 5 m depth on a fore reef site on the southwest side of Butaritari atoll (equivalent to site BUT4 in *Carilli et al.* [2012]). Following core removal, the drill hole was sealed with a precast concrete plug to prevent colonization of the inside of the coral by boring organisms and to allow coral regrowth. The core was drilled vertically to capture the maximum growth axis.

An ~6 mm thick slab was removed from the middle of the core and X-rayed to reveal annual density banding. The maximum growth axis was identified and targeted for geochemical sampling using a micromill and sample ledge approach described by *Gagan et al.* [1994] (Figure 2). Slabs and sampling ledges were cleaned thoroughly in MilliQ water using a Branson 450 ultrasonic probe, and left to air-dry for at least 24 h. After cleaning, samples were milled every 0.53 mm along the upper 23.5 cm of the core, then every 0.5 mm along the remaining 37 cm of the core (a change in motor calibration caused the slight spacing difference between sections). Every fourth sample was analyzed for both Sr/Ca and δ^{18}O (approximately bimonthly resolution) along the majority of the core. Every second sample was ultimately analyzed (approximately monthly resolution) adjacent to the thin sections in two batches: first every fourth sample, and then every second sample between these, to test if analytical errors were the origin of a Sr/Ca spike identified in the record (see 2.3 Sr/Ca analyses; Figure 2).

2.3. Sr/Ca Analyses

Coral samples for Sr/Ca analysis were weighed (between 0.5 and 1.0 mg) using a microbalance and placed into acid-washed vials. Samples were dissolved with 1% HNO_3 (Merck Suprapur) using an adjustable Eppendorf pipette to obtain an ~35 ppm final Ca concentration for optimal analysis on a Varian Vista-PRO Simultaneous inductively coupled plasma optical emission spectrometer at the Australian Nuclear Science and Technology Organization (ANSTO). Blank vials with 1% HNO_3 solution were analyzed before each sample batch to test for contamination. An internal reference solution was
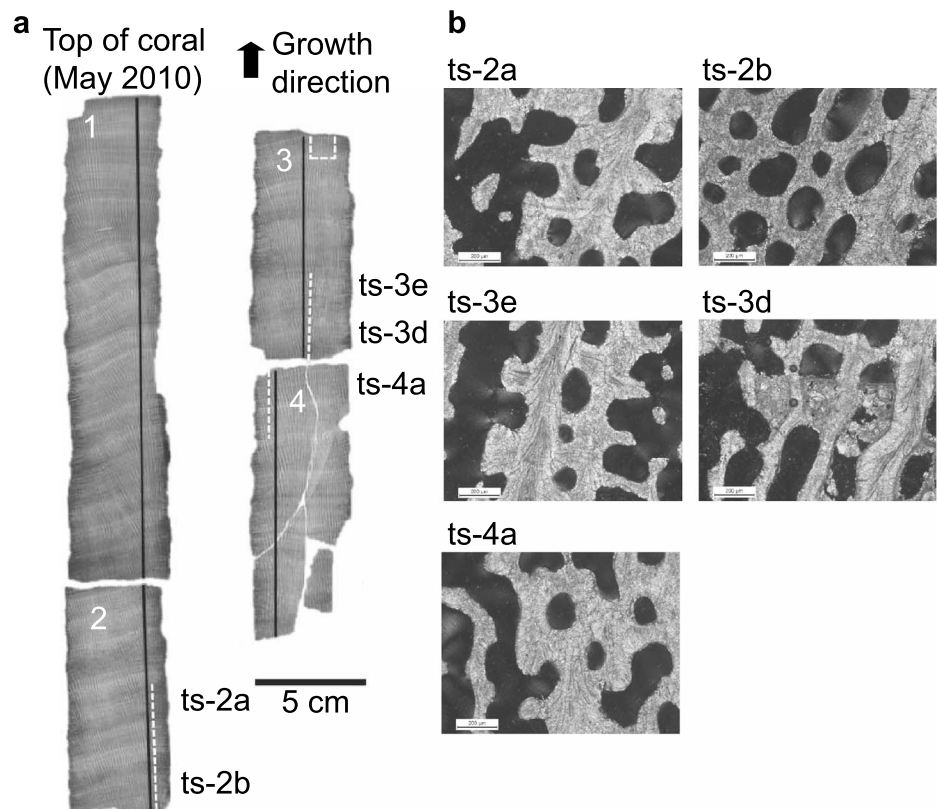
Figure 2. (a) X-radiograph positive image of the *Porites* coral core from Butaritari. Black lines show the locations of milling ledges along the major axis of coral growth. White dashed lines show locations of thin sections used to assess the degree of preservation of coral aragonite. Single dashed lines indicate thin sections taken on edge of the off-cut facing the milled ledge. The dashed box on piece 3 indicates a thin section removed from the face of the slab. Labels are the approximate locations of thin section images in Figure 2b. (b) Representative thin section images of the Butaritari coral. All images show excellent preservation of the coral. Image ts-3d shows a borer trace.

analyzed after every two coral samples to monitor and correct for machine drift during each run. The JCp-1 coral reference material [*Okai et al.*, 2002; *Hathorne et al.*, 2013] was also run with the samples, and a correction was made back to the ANSTO mean laboratory JCp-1 value of 8.811 ± 0.014 mmol/mol. The standard deviation of repeat JCp-1 analyses was 0.038 mmol/mol ($n = 12$). For some samples, Sr/Ca ratios were measured in duplicate or triplicate on the same digested solution. The average standard error (SE) for these repeat sample solutions within multiple runs was 0.011 mmol/mol ($n = 105$). Errors associated with reproducibility (or "signal/age model" errors) were computed following the methods of *Stevenson et al.* [2013], using cores from Amedee, New Caledonia [*Stephans et al.*, 2004] (supporting information). The resulting uncertainty was 0.045 mmol/mol.

An anomalous positive Sr/Ca spike was observed in samples from the top of piece 4 of the Butaritari coral core (Figure 2). Thin section analysis of this region revealed the trace of a boring organism [*McGregor and Gagan*, 2003; *McGregor and Abram*, 2008] on the face of the slab (Figure 2). On detailed inspection, the borer trace was also visible to the naked eye and tracks through coral piece 4, corresponding with the anomalous positive Sr/Ca spike. These anomalous data (equivalent to approximately 3 months in the year 1967 A.D.) were subsequently removed. Analysis of four additional thin sections from other parts of the coral core showed pristine preservation of the coral skeleton (Figure 2).

2.4. Oxygen Isotope Analyses

δ^{18}O was analyzed at the Australian National University (ANU) on a Finnigan MAT 251 mass spectrometer. For each sample, 200 ± 20 μg of powder was weighed out into a glass thimble. On the rare occasion when too
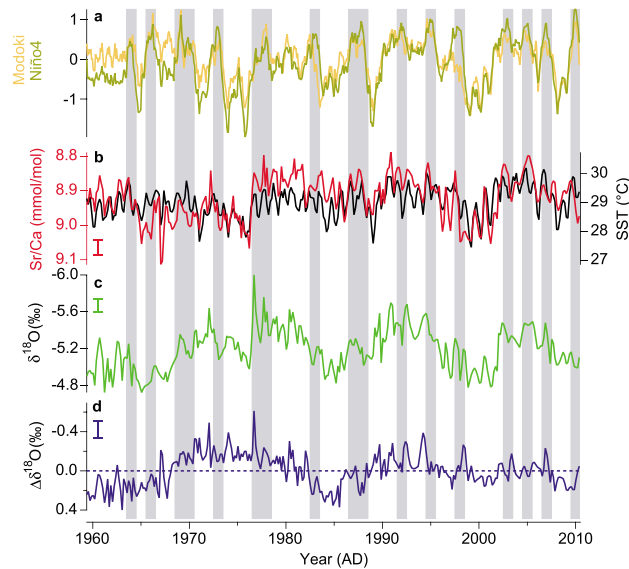
Figure 3. Comparison of the Butaritari coral geochemical records and El Niño–Southern Oscillation (ENSO) indices for the central equatorial Pacific. Coral chronology constructed by tying each annual Sr/Ca maximum to each annual coolest point in the SST record. (a) The El Niño Modoki [*Ashok et al.*, 2007] and Niño4 indices [*Rayner et al.*, 2003] for the period 1960–2010; (b) Butaritari coral Sr/Ca and SST from the ERSSTv3b data set for the grid cell centered on 4°N 172°E [*Smith et al.*, 2008], with coral Sr/Ca scaled to SST using equation (1); (c) Butaritari coral $\delta^{18}O$; and (d) Butaritari coral $\Delta\delta^{18}O$. Gray bars show El Niño events defined by the NOAA Climate Prediction Center Oceanic Niño Index (http://www.cpc.ncep.noaa.gov/products/analysis_monitoring/ensostuff/ensoyears.shtml). Error bars in Figures 3b–3d represent reproducibility based on multiple coral time series from individual locations, using data from and following methods of *Stephans et al.* [2004], *Cahyarini et al.* [2008], and *Stevenson et al.* [2013].

little coral material remained in a sample due to the previous Sr/Ca analysis, the neighboring sample (representing coral growth during the previous or following fortnight) was analyzed instead. The sample powders were then dissolved in 105% H_3PO_4 at 90°C in an automated Kiel carbonate device. National Bureau of Standards (NBS)-19 ($\delta^{18}O = -2.20‰$) and NBS-18 ($\delta^{18}O = -23.0‰$) standards were used to calibrate the isotope results relative to the Vienna Peedee Belemnite (V-PDB). The standard deviation for in-run measurements of NBS-19 was 0.04‰ ($n = 108$) for $\delta^{18}O$ during the course of the analyses. The average standard error of the mean for repeat measurements on sample aliquots within multiple runs was 0.05‰ ($n = 5$). The error calculation of *Stevenson et al.* [2013] was used to estimate the uncertainty associated with intercoral variations at a given site; using core data from New Caledonia, Rarotonga, and Kiritimati detailed in *Stevenson et al.* [2013], the resulting signal/age model error is 0.13‰ (supporting information).

2.5. Age Model

A detailed chronology was assigned to the geochemical data by tying the Sr/Ca data to monthly SST from the 2° × 2° grid square centered on 4°N, 172°E from the extended reconstructed SST version 3b (ERSSTv3b) data product [*Smith et al.*, 2008; http://www.esrl.noaa.gov/psd]. We choose the ERSSTv3b SST product for calibration and comparison, rather than HadSST3, because the ERSSTv3b data are more continuous (Figure S1 in the supporting information). Annual Sr/Ca maxima were tied to the coolest points in the SST record using Analyseries [*Paillard et al.*, 1996]. The resulting spacing of Sr/Ca data remained relatively constant throughout the record, and the chronology was verified against growth band counts from the X-radiograph. After converting depth to time in Analyseries, Sr/Ca were interpolated to six equally spaced samples per year using ARAND time series analysis software [*Howell*, 2001], corresponding to bimonthly resolution for the length of the record. Constructing the age model by tying Sr/Ca to the long-term average coldest month (February) did not significantly change the correlation between Sr/Ca and SST or ENSO indices (Figure S2 in the supporting information). The Sr/Ca depth-to-time Analyseries conversion was applied to the coral $\delta^{18}O$ data, and the $\delta^{18}O$ data were also interpolated to bimonthly resolution.
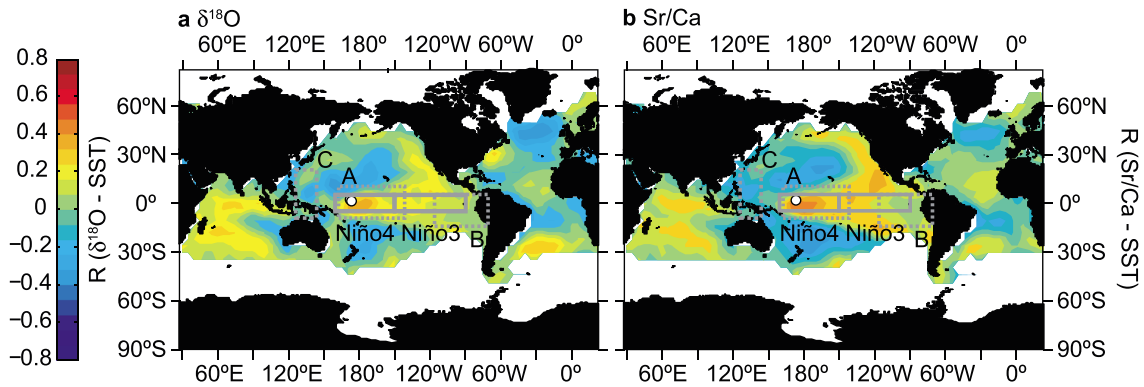
3. Results

The full Butaritari coral Sr/Ca and $\delta^{18}O$ (Figures 3b and 3c) are well correlated with SST from the 2° × 2° grid cell centered on 4°N, 172°E in ERSSTv3b ($R = -0.58$ for Sr/Ca and -0.39 for $\delta^{18}O$, $p < 0.05$ on detrended bimonthly data). Notably, the Sr/Ca time series in particular captures the amplitude of decadal SST variability observed in the instrumental data (Figure 3a).

We calibrated Sr/Ca to ERSSTv3b using the average slope of -0.084 mmol/mol/°C derived specifically to estimate interannual and decadal climate variability and twentieth century trends [*Gagan et al.*, 2012]. The

Figure 4. (a, b) Spatial correlation maps for the inverse of Butaritari coral δ^{18}O and Sr/Ca and gridded SST anomalies [*Kaplan et al.*, 1998] from 1960 to 2010. The white circle shows the approximate location of Butaritari. Solid gray boxes show the Niño3 and Niño4 SST regions [*Rayner et al.*, 2003] and dashed gray boxes the El Niño Modoki index region [*Ashok et al.*, 2007]. Note that box A SSTs become warmer and box B and C SSTs become cooler during central Pacific El Niño Modoki events [*Ashok et al.*, 2007]. The maps demonstrate that SST variability captured by the Butaritari coral records is strongly controlled by ENSO variability.

intercept (b) is then derived by solving the standard equation $SST = (m \times Sr/Ca_{mmol/mol}) + b$, where SST and Sr/Ca are the average values for the 1990–2010 calibration interval and m is -0.084 mmol/mol/°C. This results in the calibration equation:

$$SST = \left(-11.9 \times Sr/Ca_{mmol/mol}\right) + 135.3 \tag{1}$$

Over 1990–2010 $R = 0.68$ for Sr/Ca$_{SST}$ and ERSSTv3b (4°N, 172°E). Applying equation (1) to the full Sr/Ca record shows a mismatch of 0.6°C between Sr/Ca-SST and ERSSTv3b between 1976 and 1985. The coral in this interval is pristine (based on thin section analysis) and likely represents a real difference between local SSTs at Butaritari and the grid cell average ERSSTv3b data product.

We removed the SST-controlled component from the Butaritari coral δ^{18}O record to calculate the residual δ^{18}O ($\Delta\delta^{18}$O, Figure 3d), a proxy for seawater δ^{18}O, using the centering method described in *Cahyarini et al.* [2008]:

$$\Delta\delta^{18}O_{center} = \left(\delta^{18}O_i - mean\ \delta^{18}O\right) - \gamma_1/\beta_1 * \left(Sr/Ca_i - mean\ Sr/Ca\right) \tag{2}$$

where $\Delta\delta^{18}O_{center}$ is the effect of changes in seawater δ^{18}O on the coral δ^{18}O, $\delta^{18}O_i$ is measured coral δ^{18}O at each timepoint i, Sr/Ca$_i$ is measured coral Sr/Ca at each time point i, γ_1 is the coral δ^{18}O-SST regression slope of -0.22‰/°C [*Gagan et al.*, 2012], and β_1 is the coral Sr/Ca-SST slope of -0.084 mmol/mol/°C. The signal/age model error on $\Delta\delta^{18}$O was estimated as 0.175‰ by adding the Sr/Ca and δ^{18}O errors in quadrature; however, due to covariance between SST and SSS at Butaritari, the true error is likely lower (supporting information).

The Butaritari coral Sr/Ca and δ^{18}O are strongly influenced by central Pacific ENSO events, as reflected by similar low-frequency variability in the coral geochemical records and central Pacific ENSO indices (Figure 3). Indeed, field correlations show that the inverse of Sr/Ca and δ^{18}O are strongly positively correlated with SST to the southeast of Butaritari (Figure 4), roughly coinciding with the Niño4 region [*Rayner et al.*, 2003] and one of the key regions used to compute the El Niño Modoki index [*Ashok et al.*, 2007]. The SST correlation patterns in Figure 4 more closely resemble the "Modoki" El Niño than the canonical "Eastern Pacific" El Niño structure.

Spectral analysis shows that Sr/Ca$_{SST}$, δ^{18}O, and $\Delta\delta^{18}$O are dominated by decadal and longer-scale variability, with less prominent peaks at ~2.5 years in the Sr/Ca$_{SST}$ and δ^{18}O data, consistent with ENSO frequencies [*Wang*, 2000] (Figure 5). The annual cycle is more clearly resolved in the Sr/Ca$_{SST}$ data, probably because rainfall at Butaritari is not as strictly seasonal as SST variability (Figure 6). Correlations between time series of several ENSO indices (El Niño Modoki, Niño4, Niño3, and the Southern Oscillation Index) at the bimonthly scale also show that the Butaritari coral is more responsive to central Pacific warm events than canonical El Niño and La Niña events, though both are captured (Figure 7).

In addition to relationships with SST, detrended bimonthly Sr/Ca$_{SST}$ and δ^{18}O show significant correlations (Figure 7) with central Pacific ENSO indices (Niño4, *Rayner et al.* [2003], $R = 0.39$ and -0.31, respectively; El Niño Modoki index, *Ashok et al.* [2007], $R = 0.42$ and -0.31, respectively), and a salinity reconstruction (*Delcroix et al.* [2011], $R = -0.41$ and 0.24, respectively). Detrended bimonthly Sr/Ca$_{SST}$ was also weakly
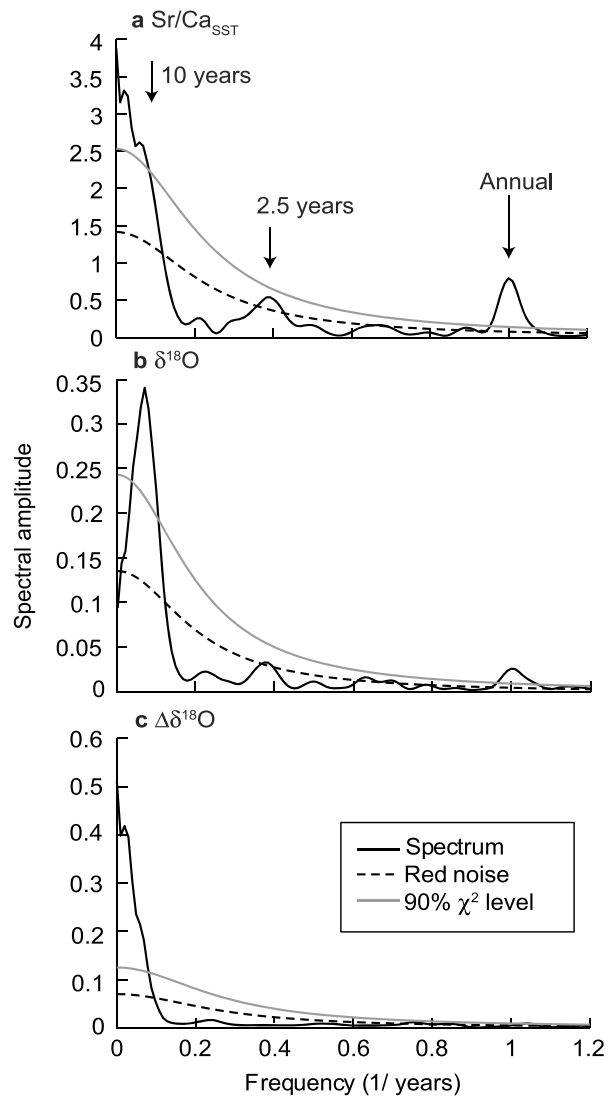
Figure 5. Spectra of the Butaritari coral geochemical records. (a) Sr/Ca$_{SST}$, (b) δ^{18}O, and (c) $\Delta\delta^{18}$O spectra (black), computed using REDFIT program for MATLAB and a Hanning window (REDFIT available at http://www.geo.uni-bremen.de/geomod/staff/mschulz/#software2) [*Schulz and Mudelsee*, 2002]. Red noise (AR(1); dashed line) and 90% chi-square (gray) confidence levels are shown. All three records are dominated by decadal-scale variability, and Sr/Ca$_{SST}$ and δ^{18}O show high-frequency ENSO variability around 2.5 years, and have an annual peak reflecting seasonal SST change.

correlated with the Niño3 index (*Rayner et al.* [2003], $R = 0.25$). Both δ^{18}O and Sr/Ca$_{SST}$ records were weakly correlated with the North Pacific Gyre Oscillation (NPGO, *Di Lorenzo et al.* [2008], $R = -0.22$ and 0.26, respectively) and Sr/Ca$_{SST}$ was weakly correlated with the Pacific Decadal Oscillation (PDO, *Mantua et al.* [1997], $R = 0.24$). The detrended bimonthly $\Delta\delta^{18}$O data were only weakly correlated with the Pacific Warm Pool index, a measure of the extent of the WPWP (WP, Martin P. Hoerling personal communication with Earth System Research Laboratory, $R = 0.21$). Reported correlation coefficients for unfiltered data all have a significance value of <0.05 calculated with the *corrcoef* function in MATLAB. In filtered data sets, degrees of freedom are reduced, and therefore, correlation coefficients must be larger to be significant; critical correlation coefficients were estimated using a white-noise null hypothesis by generating 500 white-noise time series using *randn* in MATLAB, filtering using the same 2–7 year band-pass and 9 year low-pass methods as with the geochemical and climate data, correlating pairs of filtered white-noise series and calculating the resulting 90th and 95th percentiles.

4. Discussion

4.1. Climate Variability Captured by the Butaritari Coral Record

The Butaritari coral Sr/Ca$_{SST}$, δ^{18}O, and $\Delta\delta^{18}$O record tropical Pacific climate at a range of frequencies (Figure 7) reflecting the variety of spatial and temporal climate processes affecting the region (Figures 3–6). Butaritari coral Sr/Ca$_{SST}$ correlates most strongly with the Niño3 and Niño4 indices [*Rayner et al.*, 2003] and the El Niño Modoki index [*Ashok et al.*, 2007] and captures the variability of these parameters on bimonthly, 2–7 years band pass-filtered and >9 years low pass-filtered scales (Figure 7). At frequencies longer than 9 years, Butaritari Sr/Ca$_{SST}$ and δ^{18}O capture Pacific decadal variability, reflected in strong correlations between filtered Sr/Ca$_{SST}$ and δ^{18}O and the PDO index [*Mantua et al.*, 1997] and the Pacific Warm Pool (WP) index (Figure 7).
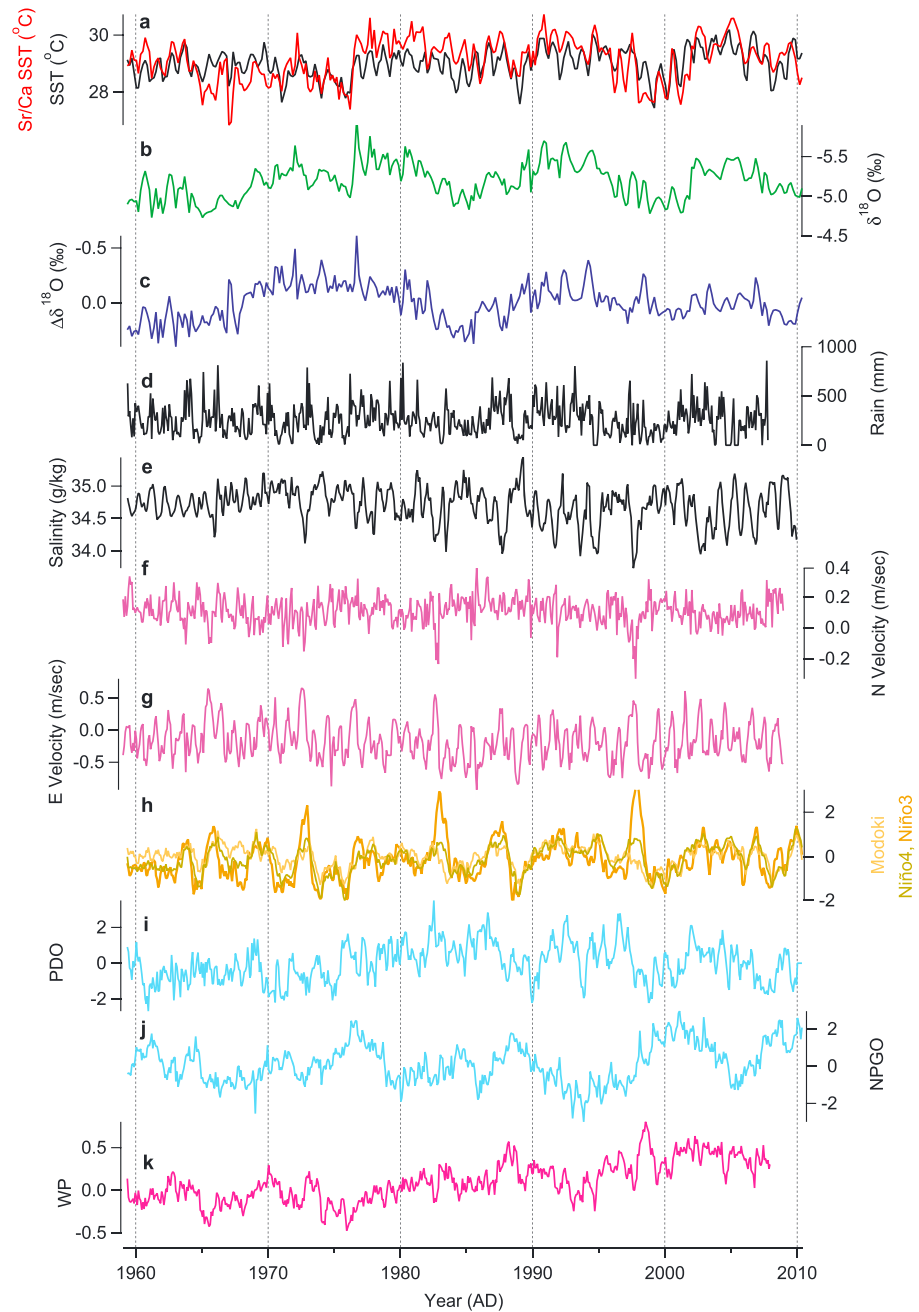
Correlations with ENSO depend strongly on the frequency band of interest. In contrast to relationships on unfiltered bimonthly data, in the 2–7 year band pass-filtered data, Sr/Ca$_{SST}$ and δ^{18}O are correlated similarly with all the ENSO SST-based indices (El Niño Modoki, Niño4, and Niño3, Figure 7). The differences in correlation strength in different frequency bands may be due to increased signal-to-noise in the filtered time series [*S. McGregor et al.*, 2013], or the possibility that on shorter timescales, SST and SSS are influenced by other processes.

Figure 6. Comparison of the Butaritari coral records with local and regional climatic records and indices. (a) Butaritari coral Sr/Ca$_{SST}$ and ERSSTv3b SST for the grid cell centered on 4°N, 172°E [*Smith et al.*, 2008]; (b) Butaritari δ^{18}O and (c) $\Delta\delta^{18}$O; (d) local rainfall measured at the Kiribati Meteorological Office; (e) sea surface salinity [*Delcroix et al.*, 2011] for the grid cell centered on 3°N 173°E; (f) northward (N) and (g) eastward (E) current velocities from the Simple Ocean Data Assimilation reanalysis [*Carton and Giese*, 2008] for the grid cell centered on 3.25°N 172.25°E; (h) the El Niño Modoki [*Ashok et al.*, 2007], Niño3 [*Trenberth*, 1997], and Niño4 [*Rayner et al.*, 2003] indices; (i) the Pacific Decadal Oscillation (PDO) index [*Mantua et al.*, 1997]; (j) the North Pacific Gyre Oscillation (NPGO) index [*Di Lorenzo et al.*, 2008]; and (k) the Warm Pool (WP) index (M. P. Hoerling, personal communication to NOAA Earth System Research Laboratory, available at http://www.esrl.noaa.gov/psd/data/climateindices/list/).

Surprisingly, without considering lag effects, the Butaritari coral records showed weak correlations with the Southern Oscillation Index (SOI), a measure of atmospheric ENSO variation, and insignificant correlations with the WP index (in bimonthly and 2–7 years band-passed data). Butaritari is located at the edge of the WPWP, and SST and SSS at Butaritari should vary along with the WPWP expansion
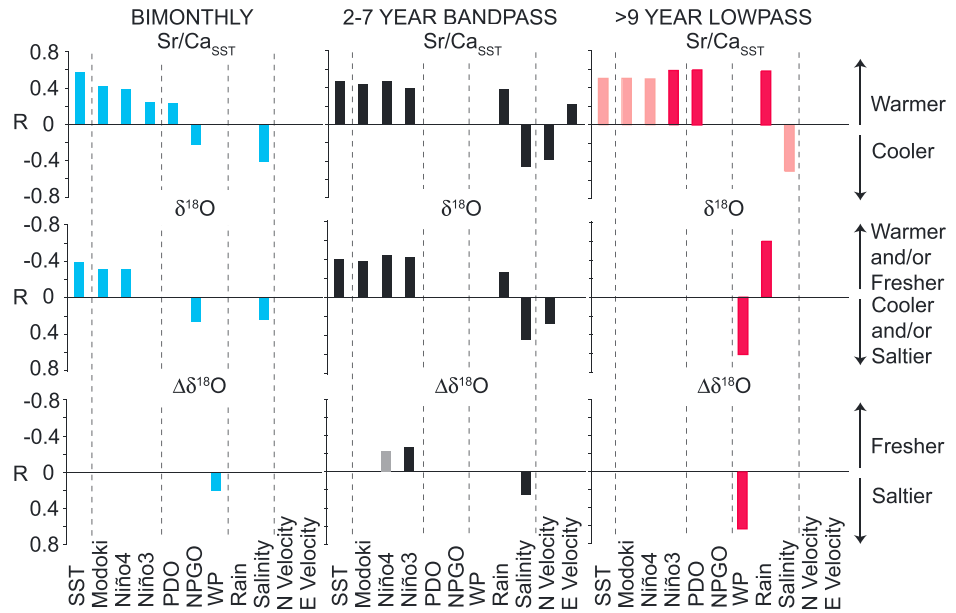
Figure 7. Summary of correlation coefficients for the Butaritari coral records and local and regional climatic records and indices. The arrows on the right describe water temperature and salinity conditions at Butaritari. The detrended bimonthly (blue), 2–7 year band pass-filtered (black), and >9 year low pass-filtered (red) Butaritari Sr/Ca$_{SST}$, δ^{18}O, and $\Delta\delta^{18}$O records for 1960 to 2010 (based on data in Figures 3 and 6) are compared with ERSSTv3b [*Smith et al.*, 2008] (SST); the El Niño Modoki index [*Ashok et al.*, 2007] (Modoki); the Niño4 index [*Rayner et al.*, 2003]; the Niño3 index [*Rayner et al.*, 2003]; the Pacific Decadal Oscillation index [*Mantua et al.*, 1997] (PDO); the North Pacific Gyre Oscillation [*Di Lorenzo et al.*, 2008] (NPGO); the Warm Pool index (WP); rainfall at Butaritari from the Kiribati Meteorological Service (Rain); sea surface salinity [*Delcroix et al.*, 2011]; and northward (N Velocity) and eastward (E Velocity) current velocities from the Simple Ocean Data Assimilation reanalysis [*Carton and Giese*, 2008]. Bars are shown for significant (dark shading: $p < 0.05$; light shading: $p < 0.10$) correlation coefficients (R) exceeding ±0.2 with no lead or lag. The bimonthly, 2–7 year band pass-filtered Butaritari coral Sr/Ca$_{SST}$ and δ^{18}O records and >9 year low pass-filtered Butaritari coral Sr/Ca$_{SST}$ records all correlate well with ENSO indices. Decadal-scale variability is reflected in strong correlations between the PDO and Sr/Ca$_{SST}$, and the WP index and δ^{18}O and $\Delta\delta^{18}$O.

and contraction during ENSO events. Further investigation revealed the strongest relationships between the geochemical records and the WP index when the geochemical records lead by 8–10 months, and the strongest correlation with the SOI when the geochemical records lag by 8–10 months (Table 2). We also checked for lagged relationships between the ERSSTv3b data product for the grid cell containing Butaritari with the SOI and WP indices and found similar relationships, suggesting that the Butaritari coral is faithfully recording the delayed response of the ocean to atmospheric initiation of El Niño (Table 2). On these timescales, after El Niño development, when Butaritari waters become warmer and fresher, the WP index increases 8–10 months later, likely reflecting first expansion of the WPWP to the east (warming at Butaritari) and then contraction back to the west (and cooling at Butaritari). Similarly, SST warming at Butaritari probably lags behind changes in the SOI because of the delay associated with propagation of warm waters to the east during El Niño following atmospheric perturbations that relax the trade winds.

Interestingly, the Butaritari coral records support earlier work from nearby Tarawa and Maiana, providing added insight into ENSO dynamics by separating the influence of water temperature and salinity on coral δ^{18}O. For example, none of the Gilbert Islands corals (Tarawa [*Cole et al.*, 1993], Maiana [*Urban et al.*, 2000], Butaritari, this work) record the large 1982–1983 canonical El Niño event, and our Butaritari record suggests this is because there was neither significant warming nor rainfall in the islands during that event (Figure 3).

Increases in salinity in the grid cell centered on Butaritari [*Delcroix et al.*, 2011], which typically occur during La Niña events, are also correlated with geochemical proxies for saltier and cooler conditions at Butaritari (Figure 7). However, given that Butaritari rainfall and salinity are not well correlated, some care must be taken in interpreting $\Delta\delta^{18}$O changes in terms of precipitation. Some of the $\Delta\delta^{18}$O signal may relate to changes in the isotopic composition of local rainfall or advection of water masses with varying δ^{18}O; the latter effect is known to be important for some sites in the South Pacific Convergence Zone [*Quinn et al.*, 1998].

Table 2. Correlation Coefficients (R) for 2–7 Year Band Pass-Filtered Geochemical Records, the Southern Oscillation Index (SOI), the Warm Pool Index (WP), and Sea Surface Temperature Estimate From ERSSTv3b Grid Cell Centered on 4°N, 172°E (SST)[a]

	Sr/Ca$_{SST}$ (R)	Lag (Months)	δ^{18}O (R)	Lag (Months)	$\Delta\delta^{18}$O (R)	Lag (Months)	SST (R)	Lag (Months)
SOI	−0.49 (0.09)	10	0.49 (0.01)	10	0.32 (0.11)	8	−0.68 (0.11)	10, 12
WP	0.48 (0.05)	−8	−0.41 (−0.16)	−8	−0.18 (−0.14)	−8	0.61 (0.23)	−8

[a]Coefficients reported are the highest computed over a range of lags from −12 to +12 months, calculating using the function *xcorr* in MATLAB. Correlations larger than the 0.19 critical value estimated with the Monte Carlo procedure described in the main text are significant. Lags associated with the highest correlation coefficient are reported in months, with the geochemical records lagging the climate records for positive lags and leading for negative lags. If multiple lags are presented, the correlation coefficient was the same for both lags. Coefficients at zero lag in parentheses.

A full understanding of Butaritari seawater δ^{18}O changes would require a mass balance approach [*Stevenson et al.*, 2013], but data limitations make such an approach extremely difficult at present. What is clear is that on interannual timescales, the Butaritari coral is responding to ENSO dynamics affected by WPWP variability, in particular the development of weak or central Pacific centered warm ENSO events or the transition between El Niño and La Niña events.

Karnauskas and Cohen [2012] found that under a warming climate, the equatorial undercurrent (EUC) should strengthen, providing a potential thermal refuge for corals in the Gilbert Islands, reducing the likelihood of coral bleaching. However, the Butaritari coral geochemical records do not show a strong correlation with current velocity (Figure 7). This could indicate that strengthening in the EUC has not occurred, at least at 3.2°N latitude, that the coral records are not strongly affected by current velocities (Figure 7), or the coral may not be deep enough to detect EUC changes (the coral is at 5 m water depth).

Another feature of the Butaritari coral records is strong decadal-scale variability in all three geochemical metrics (Figure 6). The >9 year low pass-filtered Sr/Ca$_{SST}$, δ^{18}O, and $\Delta\delta^{18}$O are all correlated with various ENSO indices and/or the WP index (Figure 7), suggesting that the decadal variability in our Butaritari coral is also related to decadal-scale variability in ENSO and WPWP dynamics. Similar decadal-scale variability in Pacific climate proxies has been identified in other coral records [*Cobb et al.*, 2001; *Holland et al.*, 2007; *Ault et al.*, 2009; *Nurhati et al.*, 2011]. Indeed, on these longer scales, the Butaritari records are equally or more strongly correlated with Niño3 than central Pacific ENSO indices and also correlated with the PDO (Figure 7). There is evidence that the mean state of the Pacific (captured by the PDO) regulates whether El Niño development stalls in the central Pacific (during PDO cool phases), or continues eastward to produce canonical El Niño events (during PDO warm phases) [*Verdon and Franks*, 2006] and that central Pacific El Niño events drive decadal changes in the NPGO [*Di Lorenzo et al.*, 2010]. The Butaritari coral records seem to reflect these phenomena, with strong links to ENSO indices and the PDO but not the NPGO on long timescales.

4.2. Evidence for a Weakening Walker Circulation

The bimonthly, interannual, and decadal-scale variability in the Butaritari coral records is superimposed on long-term trends, also identified in other coral records for the equatorial Pacific (Figure 8 and Table 3) [*Cole et al.*, 1993; *Evans et al.*, 1998; *Guilderson and Schrag*, 1999; *Urban et al.*, 2000; *Nurhati et al.*, 2009, 2011; *McGregor et al.*, 2011; *H. V. McGregor et al.*, 2013; *Cobb et al.*, 2013]. Coral δ^{18}O records for the Gilbert Islands (Tarawa [*Cole et al.*, 1993]; Maiana [*Urban et al.*, 2000], and Butaritari, this work) and Nauru [*Guilderson and Schrag*, 1999] consistently show a trend toward lower values toward the present (Figure 8 and Table 3). This trend is also observed in records for the Line Islands [*Nurhati et al.*, 2009, 2011; *Cobb et al.*, 2013], though the magnitude of the trend differs between the two regions.

The individual coral records span different time intervals, so two common intervals were selected to compare trends: (1) 1972–1998, the maximum range of available coral Sr/Ca and δ^{18}O data and (2) 1972–1990, the common interval for the majority of available coral δ^{18}O data. Over the common interval of 1972–1998, there was no significant trend in δ^{18}O at Butaritari, but significant trends toward lower δ^{18}O values in the Line Islands (Figure 8a and Table 3). Over the shorter common interval 1972–1990, trends (calculating the slope of the regression over 1972–1990 and multiplying by 18 years) of δ^{18}O at the Line Islands range from −0.11‰ to −0.29‰. The Tarawa and Maiana coral records also show trends toward lower values (−0.28‰ and −0.17‰, respectively), but δ^{18}O values in the Butaritari coral record increase by 0.20‰. Bearing in mind that the records cover different time periods, the island-group average trend in δ^{18}O for 1959–2010 (calculating the slope of the regression over the entire length of each record and multiplying by 51 years) was −0.11‰ in the Gilbert Islands and −0.66‰ in the Line Islands (Figure 8).
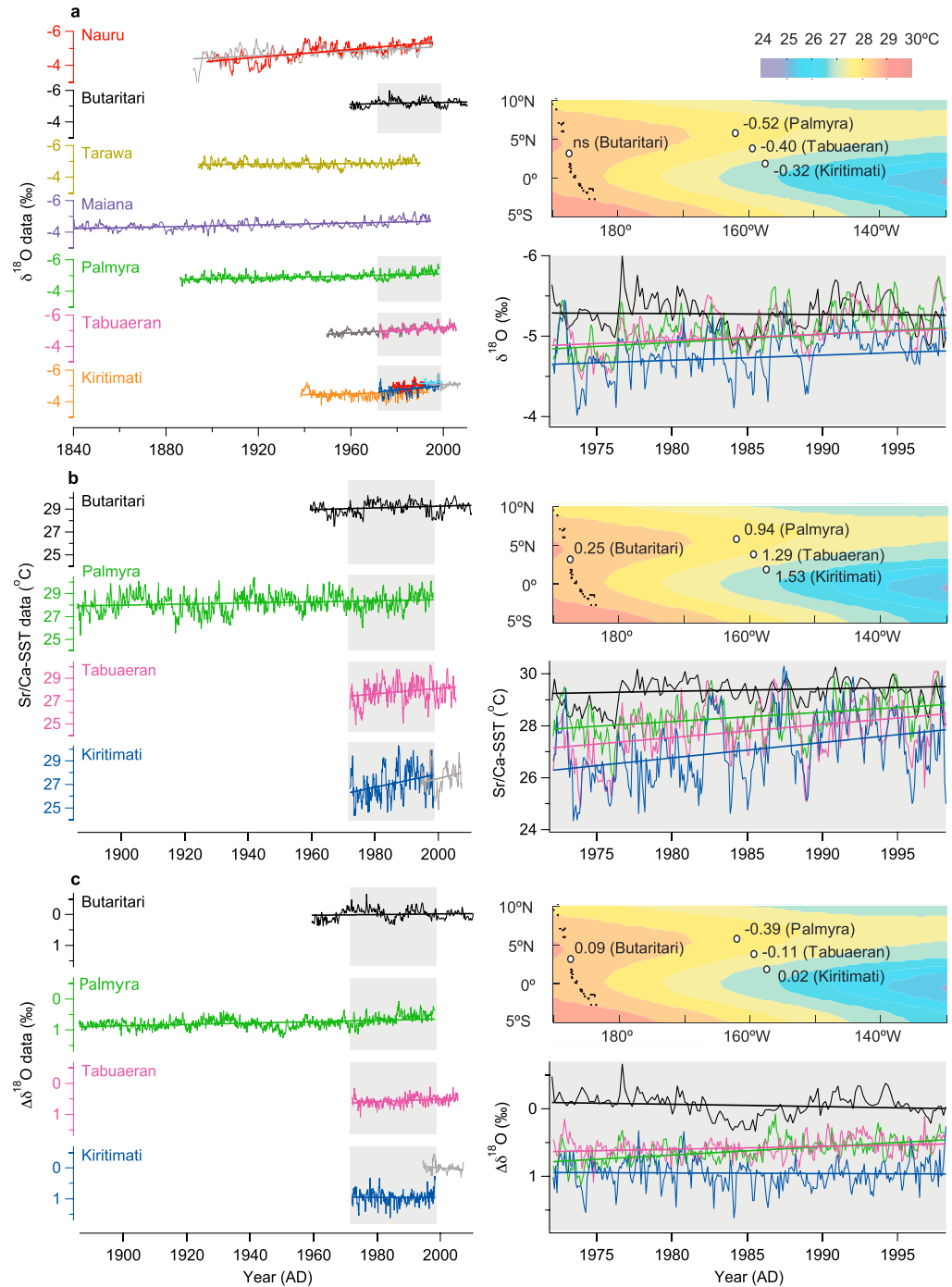
Figure 8. Summary of long-term trends in SST and SSS given by coral geochemical records for the western and central equatorial Pacific. (a) Comparison of long-term trends in coral $\delta^{18}O$ records for Nauru [*Guilderson and Schrag*, 1999] (gray and red); the Gilbert Islands: Butaritari (this study; black), Tarawa [*Cole et al.*, 1993] (olive), and Maiana [*Urban et al.*, 2000] (purple); and the Line Islands: Palmyra [*Nurhati et al.*, 2009, 2011] (green), Tabuaeran ([*Nurhati et al.*, 2009] pink and [*Cobb et al.*, 2013] gray), and Kiritimati ([*Evans et al.*, 1998] orange, [*Nurhati et al.*, 2009], dark blue, [*Woodroffe and Gagan*, 2000] red, [*Woodroffe et al.*, 2003] light blue and [*McGregor et al.*, 2011] gray). Slope values were determined by linear Kendall-Thiel fits to prewhitened data ("ns" denotes a nonsignificant trend). Right-hand plot shows trends in $\delta^{18}O$ over the common interval 1972–1998 in corals from Butaritari (western equatorial Pacific) and the Line Islands [*Nurhati et al.*, 2009] (central equatorial Pacific). Maps summarize changes in $\delta^{18}O$ recorded by each coral from 1972 to 1998, with the spatial distribution of annual average SSTs shown for context. (b, c) As for Figure 8a but for coral Sr/Ca_{SST} and $\Delta\delta^{18}O$. The coral records from the Line Islands (central equatorial Pacific) show enhanced warming and freshening compared with the Gilbert Islands (western equatorial Pacific), suggesting a reduction in east-west SST and SSS gradients.

Table 3. Slopes of Kendall-Thiel Fits to Coral Geochemical Data Sets[a]

Island	$\delta^{18}O$	Sr/Ca$_{SST}$	$\Delta\delta^{18}O$
	Slopes Over Entire Records		
Nauru (gray)[b]	−0.007		
Nauru (red)[b]	−0.011		
Butaritari[c]	−0.003	0.008	−0.001
Tarawa[d]	−0.001		
Maiana[e]	−0.003		
Palmyra[f]	−0.003	0.005	−0.002
Tabuaeran (gray)[g]	−0.009	0.036	−0.004
Tabuaeran (pink)[f]	−0.01		
Kiritimati (orange)[h]	−0.003		
Kiritimati (red)[i]	−0.009		
Kiritimati (dark blue)[f]	−0.013	0.057	ns
Kiritimati (light blue)[j]	−0.016		
Kiritimati (gray)[k,l]	ns	0.067	0.009
	Slopes Over 1972–1998		
Butaritari[c]	ns	0.010	0.004
Palmyra[f]	−0.020	0.036	−0.012
Tabuaeran[f]	−0.015	0.050	−0.004
Kiritimati[f]	−0.013	0.059	ns

[a]Nonsignificant slopes are denoted with ns.
[b]*Guilderson and Schrag* [1999].
[c]This work.
[d]*Cole et al.* [1993].
[e]*Urban et al.* [2000].
[f]*Nurhati et al.* [2009].
[g]*Cobb et al.* [2013].
[h]*Evans et al.* [1998].
[i]*Woodroffe and Gagan* [2000].
[j]*Woodroffe et al.* [2003].
[k]*McGregor et al.* [2011].
[l]*H. V. McGregor et al.* [2013].

The difference in the magnitude of the $\delta^{18}O$ trends may, however, reflect site-specific contributions of SST and $\delta^{18}O_{seawater}$ to the coral $\delta^{18}O$ records, so deconvolving this signal is important. To facilitate comparison between the Butaritari and Line Islands Sr/Ca records, the Butaritari Sr/Ca was recalibrated to SST with a reduced major axis calibration (RMA; supporting information), the same method used for the Line Island corals. The RMA calibration results in Sr/Ca$_{SST}$ and $\Delta\delta^{18}O$ trends for the Butaritari records that are similar to those given by the calibration coefficients of *Gagan et al.* [2012] (Figure S3 and Table S1 in the supporting information). Over the common interval 1972–1998 the Butaritari Sr/Ca$_{SST}$ record reveals a slower rate of warming compared to the Line Islands (Figure 8 and Table 3). This zonal difference in warming trends is consistent with the warming trend in SST products. However, the ERSSTv3b SST trend at Butaritari from 1972 to 1998 (0.62°C) is larger than the coral Sr/Ca-derived SST trend (0.25°C), but this is likely influenced by the mismatch of values in ERSSTv3b compared with the Butaritari coral Sr/Ca$_{SST}$ between 1976 and 1985 mentioned in the results section. An increased rate of warming at the Line Islands compared to the Gilbert Islands suggests a reduction in the zonal (east-west) gradient in SST across the Pacific, which could reflect a weakening Walker Circulation.

The coral $\Delta\delta^{18}O$ proxy for SSS change also showed differences between Butaritari and the Line Islands; at Butaritari there was no significant trend in $\Delta\delta^{18}O$ over the entire 51 year record, while during the common 1972–1998 interval, the record shows a slight trend toward more saline conditions. The Line Islands (Palmyra, Tabuaeran, and Kiritimati) on average show larger trends toward more negative $\Delta\delta^{18}O$ (freshening) over the 1972–1998 interval and also include a latitudinal trend in $\Delta\delta^{18}O$, which *Nurhati et al.* [2009] suggest could be caused by strengthening or increased migration of the ITCZ over Palmyra. Rainfall records, however, over the common interval 1972–1998 from Butaritari and Tarawa (Gilbert Islands), and Tabuaeran and Kiritimati (Line Islands) from the Kiribati Meteorological Service showed no significant trends. This could be influenced by gaps in the rainfall records or a decoupling between rainfall and local SSS (for instance see weak correlations between rainfall and SSS proxies at Butaritari, Table 1). Overall, more freshening at the Line Islands compared to Butaritari also suggests a reduction in zonal SSS gradients and recent weakening of the Walker Circulation.

A potential factor influencing these cross-Pacific trends is that the common time interval of 1972–1998 encompasses a PDO warm phase, and apparent zonal differences might instead reflect an increase in the frequency of canonical El Niño events. *Solomon and Newman* [2012] found that cross-Pacific differences in SST trends are not significant when ENSO variability is removed from SST data products. However, cross-Pacific differences in trends in coral geochemical data are robust to >8 year low-pass filtering of the data before trend fitting (Table S2 in the supporting information; note that a >8 year low-pass filter was used to match the analysis of *Solomon and Newman* [2012]). After >8 year low-pass filtering, the coral $\Delta\delta^{18}$O record indicates a slight freshening trend at Butaritari, instead of the slight trend toward higher SSS observed before filtering, but the magnitude of freshening is still smaller than that suggested by coral $\Delta\delta^{18}$O in the Line Islands. Also, as noted above, the Butaritari coral geochemical records do reflect canonical El Niño events on long timescales (Figure 7), and when ENSO variability is removed from the records using an 8 year low-pass filter, the cross-Pacific trends remain, suggesting that the different rates of warming and freshening at the Gilbert and Line Islands are real.

Recent studies suggest that east-west SST and SSS gradients across the equatorial Pacific have changed during the late twentieth century [*Williams and Grottoli*, 2010; *Nurhati et al.*, 2011]. However, the Butaritari coral record indicates a slower rate of warming and no freshening over the past half-century at Butaritari, in contrast to the rapid warming and significant freshening indicated by coral records from the Line Islands to the east (Figure 8). Taken together, the trends in SST and SSS evident in coral records spanning the central Pacific suggest greater warming and freshening in the Line Islands to the east than in the Gilbert Islands to the west.

5. Conclusions

New coral geochemical records from Butaritari atoll in the central western equatorial Pacific, show that this region is dominated by ENSO and WPWP dynamics, with strong decadal variability. Longer-term eastward migrations of the WPWP, which bring warmer and fresher water to Butaritari, are reflected in strong correlations between coral δ^{18}O and $\Delta\delta^{18}$O on >9 years timescales. On these timescales, the PDO and NPGO also affect Butaritari Sr/Ca and $\Delta\delta^{18}$O, in contrast to coral records for the Line Islands where only Sr/Ca responds to the NPGO, and $\Delta\delta^{18}$O responds to the PDO [*Nurhati et al.*, 2011]. The different responses of the two localities suggest there may be potential to compare corals from these islands to test for changes in different types of decadal variability. The time-lag between geochemical signals in the bimonthly resolved coral records and the SOI and WP indices suggests that the Butaritari coral records transitions between ENSO phases. The new Butaritari coral records also show a reduced rate of warming and freshening during the second half of the twentieth century compared with contemporary coral records further east, suggesting a weakening of the Walker Circulation.

References

Adler, R. F., et al. (2003), The Version 2 Global Precipitation Climatology Project (GPCP) monthly precipitation analysis (1979-present), *J. Hydrometeorol.*, 4, 1147–1167.

Ashok, K., S. K. Behera, S. A. Rao, H. Weng, and T. Yamagata (2007), El Niño Modoki and its possible teleconnection, *J. Geophys. Res.*, 112, C11007, doi:10.1029/2006JC003798.

Ault, T. R., J. E. Cole, M. N. Evans, H. Barnett, N. J. Abram, A. W. Tudhope, and B. K Linsley (2009), Intensified decadal variability in tropical climate during the late 19th century, *Geophys. Res. Lett.*, 36, L08602, doi:10.1029/2008GL036924.

Beck, J. W., R. L. Edwards, E. Ito, F. W. Taylor, J. Recy, F. Rougerie, P. Joannot, and C. Henin (1992), Sea-surface temperature from coral skeletal strontium/calcium ratios, *Science*, 257, 644–647.

Cahyarini, S. Y., M. Pfeiffer, O. Timm, W.-C. Dullo, and D. G. Schönberg (2008), Reconstructing seawater δ^{18}O from paired coral δ^{18}O and Sr/Ca ratios: Methods, error analysis and problems, with examples from Tahiti (French Polynesia) and Timor (Indonesia), *Geochim. Cosmochim. Acta*, 72, 2841–2853.

Carilli, J., S. D. Donner, and A. C. Hartmann (2012), Historical temperature variability affects coral response to heat stress, *PLoS One*, 7, e34418.

Carton, J. A., and B. S. Giese (2008), A reanalysis of ocean climate using Simple Ocean Data Assimilation (SODA), *Mon. Weather Rev.*, 136, 2999–3017.

Chen, D., A. J. Busalacchi, and L. M. Rothstein (1994), The roles of vertical mixing, solar radiation, and wind stress in a model simulation of the sea surface temperature seasonal cycle in the tropical Pacific Ocean, *J. Geophys. Res.*, 99, 20,345–20,359, doi:10.1029/94JC01621.

Cobb, K. M., C. D. Charles, and D. E. Hunter (2001), A central tropical Pacific coral demonstrates Pacific, Indian, and Atlantic decadal climate connections, *Geophys. Res. Lett.*, 28, 2209–2212, doi:10.1029/2001GL012919.

Cobb, K. M., N. Westphal, H. R. Sayano, J. T. Watson, E. Di Lorenzo, H. Cheng, R. L. Edwards, and C. D. Charles (2013), Highly variable El Niño–Southern Oscillation throughout the Holocene, *Science*, 339, 67–70.

Cole, J. E., R. G. Fairbanks, and G. T. Shen (1993), Recent variability in the Southern Oscillation: Isotopic results from a Tarawa Atoll coral, *Science*, 260, 1790–1793.

Cravatte, S., T. Delcroix, D. Zhang, M. McPhaden, and L. Leloup (2009), Observed freshening and warming of the western Pacific warm pool, *Clim. Dyn.*, 33, 565–589.

Delcroix, T., and J. Picaut (1998), Zonal displacement of the western equatorial Pacific "fresh pool", *J. Geophys. Res., 103*, 1087–1098, doi:10.1029/97JC01912.

Delcroix, T., S. Cravatte, and M. J. McPhaden (2007), Decadal variations and trends in tropical Pacific sea surface salinity since 1970, *J. Geophys. Res., 112*, C03012, doi:10.1029/2006JC003801.

Delcroix, T., G. Alory, S. Cravatte, T. Corrége, and M. J. McPhaden (2011), A gridded sea surface salinity data set for the tropical Pacific with sample applications (1950–2008), *Deep Sea Res., Part I, 58*, 38–48.

Deser, C., A. S. Phillips, and M. A. Alexander (2010), Twentieth century tropical sea surface temperature trends revisited, *Geophys. Res. Lett., 37*, L10701, doi:10.1029/2010GL043321.

Di Lorenzo, E., N. Schneider, K. M. Cobb, P. J. S. Franks, K. Chhak, A. J. Miller, J. C. McWilliams, S. J. Bograd, H. Arango, and E. Curchitser (2008), North Pacific Gyre Oscillation links ocean climate and ecosystem change, *Geophys. Res. Lett., 35*, L08607, doi:10.1029/2007GL032838.

Di Lorenzo, E., K. M. Cobb, J. C. Furtado, N. Schneider, B. T. Anderson, A. Bracco, M. A. Alexander, and D. J. Vimont (2010), Central Pacific El Niño and decadal climate change in the North Pacific ocean, *Nat. Geosci., 3*, 762–765.

Donner, S. D. (2011), An evaluation of the effect of recent temperature variability on the prediction of coral bleaching events, *Ecol. Appl., 21*, 1718–1730.

England, M. H., S. McGregor, P. Spence, G. A. Meehl, A. Timmermann, W. Cai, A. Sen Gupta, M. J. McPhaden, A. Purich, and A. Santoso (2014), Recent intensification of wind-driven circulation in the Pacific and the ongoing warming hiatus, *Nat. Clim. Change, 4*, 222–227.

Evans, M. N., R. G. Fairbanks, and J. L. Rubenstone (1998), A proxy index of ENSO teleconnections, *Nature, 394*, 732–733.

Gagan, M. K., A. R. Chivas, and P. J. Isdale (1994), High-resolution isotopic records from corals using ocean temperature and mass-spawning chronometers, *Earth Planet. Sci. Lett., 121*, 549–558.

Gagan, M. K., L. K. Ayliffe, D. Hopley, J. A. Cali, G. E. Mortimer, J. Chappell, M. T. McCulloch, and M. J. Head (1998), Temperature and surface-ocean water balance of the mid-Holocene tropical western Pacific, *Science, 279*, 1014–1018.

Gagan, M. K., G. B. Dunbar, and A. Suzuki (2012), The effect of skeletal mass accumulation in *Porites* on coral Sr/Ca and δ^{18}O paleothermometry, *Paleoceanography, 27*, PA1203, doi:10.1029/2011PA002215.

Guilderson, T. P., and D. P. Schrag (1999), Reliability of coral isotope records from the Western Pacific Warm Pool: A comparison using age-optimized records, *Paleoceanography, 14*, 457–464, doi:10.1029/1999PA900024.

Hathorne, E. C., et al. (2013), Interlaboratory study for coral Sr/Ca and other element/Ca ratio measurements, *Geochem. Geophys. Geosyst., 14*, 3730–3750, doi:10.1002/ggge.20230.

Holland, C. L., R. B. Scott, S. I. An, and F. W. Taylor (2007), Propagating decadal sea surface temperature signal identified in modern proxy records of the tropical Pacific, *Clim. Dyn., 28*, 163–179.

Howell, P. (2001), *ARAND Time Series and Spectral Analysis Package for the Macintosh, Brown University*, IGBP PAGES/World Data Center Paleoclimatol. Data Contrib. Ser., vol. 44, NOAA/NGDC Paleoclimatology Program, Boulder, Colo.

Kaplan, A., M. Cane, Y. Kushnir, A. Clement, M. Blumenthal, and B. Rajagopalan (1998), Analyses of global sea surface temperature 1856–1991, *J. Geophys. Res., 103*, 18,567–18,589, doi:10.1029/97JC01736.

Karnauskas, K. B., and A. L. Cohen (2012), Equatorial refuge amid tropical warming, *Nat. Clim. Change, 2*, 530–534.

Mantua, N. J., S. R. Hare, Y. Zhang, J. M. Wallace, and R. C. Francis (1997), A Pacific interdecadal climate oscillation with impacts on salmon production, *Bull. Am. Meteorol. Soc., 78*, 1069–1079.

McCulloch, M. T., M. K. Gagan, G. E. Mortimer, A. R. Chivas, and P. J. Isdale (1994), A high-resolution Sr/Ca and δ^{18}O coral record from the Great Barrier Reef, Australia, and the 1982–1983 El Niño, *Geochim. Cosmochim. Acta, 58*, 2747–2754.

McGregor, H. V., and N. J. Abram (2008), Images of diagenetic textures in *Porites* corals from Papua New Guinea and Indonesia, *Geochem. Geophys. Geosyst., 9*, Q10013, doi:10.1029/2008GC002093.

McGregor, H. V., and M. K. Gagan (2003), Diagenesis and geochemistry of *Porites* corals from Papua New Guinea: Implications for paleoclimate reconstruction, *Geochim. Cosmochim. Acta, 67*, 2147–2156.

McGregor, H. V., M. J. Fischer, M. K. Gagan, D. Fink, and C. D. Woodroffe (2011), Environmental control of the oxygen isotope composition of *Porites* coral microatolls, *Geochim. Cosmochim. Acta, 75*, 3930–3944.

McGregor, H. V., M. J. Fischer, M. K. Gagan, D. Fink, S. J. Phipps, H. Wong, and C. D. Woodroffe (2013), A weak El Niño/Southern Oscillation with delayed seasonal growth around 4,300 years ago, *Nat. Geosci., 6*, 949–953.

McGregor, S., A. Timmermann, M. H. England, O. E. Timm, and A. T. Wittenberg (2013), Inferred changes in El Niño-Southern Oscillation variance over the past six centuries, *Clim. Past, 9*, 2269–2284.

Meng, Q., M. Latif, W. Park, N. S. Keenlyside, V. A. Semenov, and T. Martin (2012), Twentieth century Walker Circulation change: Data analysis and model experiments, *Clim. Dyn., 38*, 1757–1773.

Nurhati, I. S., K. M. Cobb, C. D. Charles, and R. B. Dunbar (2009), Late 20th century warming and freshening in the central tropical Pacific, *Geophys. Res. Lett., 36*, L21606, doi:10.1029/2009GL040270.

Nurhati, I. S., K. M. Cobb, and E. Di Lorenzo (2011), Decadal-scale SST and salinity variations in the central tropical Pacific: Signatures of natural and anthropogenic climate change, *J. Clim., 24*, 3294–3308.

Okai, T., A. Suzuki, H. Kawahata, S. Terashima, and N. Imai (2002), Preparation of a new Geological Survey of Japan geochemical reference material: Coral JCp-1, *Geostand. Newsl., 26*, 95–99.

Paillard, D., L. Labeyrie, and P. Yiou (1996), Macintosh program performs time-series analysis, *Eos Trans. AGU, 77*, 379–379.

Quinn, T. M., T. J. Crowley, F. W. Taylor, C. Henin, P. Joannot, and Y. Join (1998), A multicentury stable isotope record from a New Caledonia coral: Interannual and decadal sea surface temperature variability in the southwest Pacific since 1657 AD, *Paleoceanography, 13*(4), 412–426, doi:10.1029/98PA00401.

Rasmusson, E. M., and J. M. Wallace (1983), Meteorological aspects of the El Niño/Southern Oscillation, *Science, 222*, 1195–1202.

Rayner, N., D. E. Parker, E. B. Horton, C. K. Folland, L. V. Alexander, D. P. Rowell, E. C. Kent, and A. Kaplan (2003), Global analyses of sea surface temperature, sea ice, and night marine air temperature since the late nineteenth century, *J. Geophys. Res., 108*(D14), 4407, doi:10.1029/2002JD002670.

Ren, L., B. K. Linsley, G. M. Wellington, D. P. Schrag, and O. Hoegh-Guldberg (2003), Deconvolving the δ^{18}O seawater component from subseasonal coral δ^{18}O and Sr/Ca at Rarotonga in the southwestern subtropical Pacific for the period 1726 to 1997, *Geochim. Cosmochim. Acta, 67*, 1609–1621.

Schulz, M., and M. Mudelsee (2002), REDFIT: Estimating red-noise spectra directly from unevenly spaced paleoclimatic time series, *Comput. Geosci., 28*, 421–426.

Smith, T. M., R. W. Reynolds, T. C. Peterson, and J. Lawrimore (2008), Improvements to NOAA's historical merged land-ocean surface temperature analysis (1880–2006), *J. Clim., 21*, 2283–2296.

Solomon, A., and M. Newman (2012), Reconciling disparate twentieth-century Indo-Pacific ocean temperature trends in the instrumental record, *Nat. Clim. Change, 2*, 691–699.

Stephans, C. L., T. M. Quinn, F. W. Taylor, and T. Corrège (2004), Assessing the reproducibility of coral-based climate records, *Geophys. Res. Lett.*, *31*, L18210, doi:10.1029/2004GL020343.

Stevenson, S., H. V. McGregor, S. J. Phipps, and B. Fox-Kemper (2013), Quantifying errors in coral-based ENSO estimates: Toward improved forward modeling of δ^{18}O, *Paleoceanography*, *28*, 633–649, doi:10.1002/palo.20059.

Sun, D.-Z. (2003), A possible effect of an increase in the warm-pool SST on the magnitude of El Niño warming, *J. Clim.*, *16*, 185–205.

Tokinaga, H., S. P. Xie, C. Deser, Y. Kosaka, and Y. M. Okumura (2012), Slowdown of the Walker Circulation driven by tropical Indo-Pacific warming, *Nature*, *491*, 439–443.

Trenberth, K. E. (1997), The definition of El Niño, *Bull. Am. Meteorol. Soc.*, *78*, 2771–2777.

Urban, F. E., J. E. Cole, and J. T. Overpeck (2000), Influence of mean climate change on climate variability from a 155-year tropical Pacific coral record, *Nature*, *407*, 989–993.

Vecchi, G. A., and B. J. Soden (2007), Global warming and the weakening of the tropical circulation, *J. Clim.*, *20*, 4316–4340.

Vecchi, G. A., B. J. Soden, A. T. Wittenberg, I. M. Held, A. Leetmaa, and M. J. Harrison (2006), Weakening of tropical pacific atmospheric circulation due to anthropogenic forcing, *Nature*, *441*, 73–76.

Verdon, D. C., and S. W. Franks (2006), Long-term behaviour of ENSO: Interactions with the PDO over the past 400 years inferred from paleoclimate records, *Geophys. Res. Lett.*, *33*, L06712, doi:10.1029/2005GL025052.

Wang, B. (2000), Interdecadal change of the structure of the ENSO mode and its impact on the ENSO frequency, *J. Clim.*, *13*, 2044–2055.

Wang, H.-J., R. H. Zhang, J. Cole, and F. Chavez (1999), El Niño and the related phenomenon Southern Oscillation (ENSO): The largest signal in interannual climate variation, *Proc. Natl. Acad. Sci. U.S.A.*, *96*, 11,071–11,072.

Williams, B., and A. G. Grottoli (2010), Recent shoaling of the nutricline and thermocline in the western tropical Pacific, *Geophys. Res. Lett.*, *37*, L22601, doi:10.1029/2010GL044867.

Woodroffe, C. D., and M. K. Gagan (2000), Coral microatolls from the central Pacific record late Holocene El Niño, *Geophys. Res. Lett.*, *27*(10), 1511–1514, doi:10.1029/2000GL011407.

Woodroffe, C. D., M. R. Beech, and M. K. Gagan (2003), Mid-late Holocene El Niño variability in the equatorial Pacific from coral microatolls, *Geophys. Res. Lett.*, *30*(7), 1358, doi:10.1029/2002GL015868.